



Sodium recycling at Europa: what do we learn from the sodium cloud variability?

F. Cipriani,¹ F. Leblanc,^{2,3} O. Witasse,¹ and R. E. Johnson⁴

Received 18 June 2008; revised 5 August 2008; accepted 20 August 2008; published 7 October 2008.

[1] We study the ejection of sodium atoms from Europa's surface by both magnetospheric ion and electron sputtering and desorption stimulated by UV solar photons. The depletion of the surface by ejection and its enrichment by redeposition of sodium atoms are described. The redistribution of sodium atoms at the surface induced by photo-stimulated desorption from the dayside and by sputtering ejection from the trailing hemisphere cannot explain the observed variation of the Na emission brightness. However, a transient increase of the sputtering rate due to a plasma injection may explain such an increase. The relationship between the sodium surface content and the sodium exosphere are also discussed. **Citation:** Cipriani, F., F. Leblanc, O. Witasse, and R. E. Johnson (2008), Sodium recycling at Europa: what do we learn from the sodium cloud variability?, *Geophys. Res. Lett.*, *35*, L19201, doi:10.1029/2008GL035061.

1. Introduction

[2] A thin sodium atmosphere with a column density of 10^{10} cm^{-2} was first detected at Europa by *Brown and Hill* [1996], and studied in more detail by *Brown* [2001] and *Leblanc et al.* [2005]. Energetic heavy ions trapped in the Jovian magnetosphere efficiently sputter Europa's surface, ejecting water molecules as well as trace species such as sodium and potassium. Such ejected species have a typical lifetime of about 50 hours before ionization. They are also lost either by escaping Europa gravity field or return to the surface where they thermalize. A total of four observations (in 12/1999 and 11/2000) at different positions of Europa along its orbit, suggested a variation by a factor of five of the sodium emission intensity (see *Leblanc et al.* [2002, 2005] for an extensive description of these observations). *Leblanc et al.* [2005] suggested that such variation could be due to an increase of the ejection rate just after Europa passed through Jupiter's magnetotail and shadow, induced by the migration of sodium atoms from trailing to leading sides.

[3] In order to investigate this hypothesis, the 3D Monte Carlo model initially developed by *Leblanc et al.* [2002, 2005] has been here extended to account for the mutual influence of sputtering and photo-stimulated desorption on the global Na ejection rate and cloud morphology (section 2). Of particular interest is the period of highly enhanced sodium emission. Below we confirm that sodium cloud morphology

is well described by the processes considered by *Leblanc et al.* [2002, 2005], but that the various sources of variability examined below can not explain the large enhancement, contrary to earlier suggestions (section 3). Therefore, we propose that a large injection of energetic plasma associated with plasma storm may cause the enhanced emission.

2. Model Description

[4] The exosphere model has been described in details by *Leblanc et al.* [2002] and *Leblanc et al.* [2005]. We report here two important updates of this model.

[5] (1) In the present study, we have implemented a 2D surface grid (60×30 cells) in order to account for non-uniform Na density distribution in the icy surface. We assume an initial atomic surface density of $2 \times 10^{13} \text{ cm}^{-2}$, based on a surface concentration of $C_{\text{Na}} = 0.8\%$ [*Johnson, 2000; Leblanc et al., 2005*].

[6] (2) In the present study, we also account for the ejection of Na atoms by photo-stimulated desorption by solar UV photons. As a consequence, at each time step, the flux rate of ejected Na atoms is calculated accounting for the Na atom surface cell density, the impacting flux of ions and electrons in this cell and the flux of photons illuminating this cell.

[7] The rate of ejection of Na by electron and ion sputtering is calculated by multiplying the flux Φ of incident magnetospheric particles impacting a cell of the surface with the sputtering yield Y_{cell} and the cell area S_{cell} . The sputtering yield Y_{cell} is proportional to the sodium surface concentration C_{Na} in the cell. It is a weighted function of the yield of sputtering from pure ice Y_{ice} and the yield of sputtering from non-ice (hydrated minerals/salts bearing) materials Y_{nonice} . Following *Johnson* [2000], Y_{ice} is typically lower than 20 (here we assume it can take values between 10 and 20) and Y_{nonice} is typically larger than 1 (here we assume it can take values between 0.5 and 1). The incident flux Φ of magnetospheric ions and electrons is distributed according to $\Phi(\Theta) = A + B\cos(\Theta)$, where Θ is the angle with respect to the apex of the trailing hemisphere, A and B are adjustable coefficients accounting for the asymmetry of the incident flux between trailing and leading hemispheres [*Cassidy et al., 2007*]. In nominal conditions, the total mean incident flux of ions at Europa's surface is equal to $5 \times 10^7 \text{ cm}^{-2} \cdot \text{s}^{-1}$, in agreement with Galileo EPD measurements [*Cooper et al., 2001*]. The position of the maximum of the incident flux with respect to the apex of the trailing hemisphere (within a latitude interval of $\pm 10^\circ$ with respect to Europa equator) and its flux intensity (within a factor of 2 in amplitude) vary with Europa centrifugal latitude as in the work by *Leblanc et al.* [2005].

[8] The ejection rate of Na by photo-stimulated desorption is the product of the integrated solar UV photon flux at

¹ESTEC, ESA, Noordwijk, Netherlands.

²Service d'Aéronomie du CNRS, IPSL, Verrières Le Buisson, France.

³Now at Osservatorio Astronomico di Trieste, Trieste, Italy.

⁴Engineering Physics, University of Virginia, Charlottesville, Virginia, USA.

Table 1. Five Representative Cases^a

Parameter	Case 1	Case 2	Case 3	Case 4	Case 5
Φ (cm ⁻² .s ⁻¹)	2×10^8	2×10^8	2×10^8	2×10^8	Injection, $\Phi \times 8$
Ψ (cm ⁻² .s ⁻¹)	uniform	non uniform	uniform	uniform	uniform
Q (cm ²)	10^{-20}	10^{-20}	10^{-19}	10^{-20}	10^{-20}
Y_{ice}/Y_{nice}	20/0.5	20/0.5	20/0.5	10/0.5	20/0.5
Surface source rate (s ⁻¹)	4.67×10^{-24}	4.64×10^{-24}	5.25×10^{-24}	4.53×10^{-24}	6.62×10^{-24}

^aCase 1: nominal case. Case 2: the source term Ψ is distributed following the distribution of the non ice material from *Grundy et al.* [2007]. Case 3: one order of magnitude larger PSD cross section than case 1. Case 4: yield of sputtering from pure ice two times smaller than case 1. Case 5: local plasma injection.

Europa, times the photo-stimulated desorption cross section, the cosine of the solar zenithal angle, the surface cell area and C_{Na} . The PSD desorption cross section can vary between 1.0×10^{-20} to 1.0×10^{-19} cm² with the lower value appropriate for a rough regolith surface [*Yakshinskiy and Madey*, 1999]. Europa's surface illumination is calculated at each Europa position taking into account Europa's pass through Jupiter's shadow. Assuming the same behaviour as for sodium desorbed from refractory surfaces [*Leblanc and Johnson*, 2003], the energy distribution of the ejected sodium by PSD peaks at the same energy value (around 0.1 eV) as the energy distribution related to electronic sputtering but with a faster decreasing energetic tail.

[9] A simulated macro-particle (representing about 10^{26} real particles) is ejected by one of the mechanisms each time the associated ejection rate in a cell multiplied by the simulation time step exceeds the macro-particle numerical weight. The weight of a sputtered particle is typically set to be five times that of a photo-desorbed particle, in order to ensure sufficient statistics to simulate PSD with respect to sputtering. At each time step, each cell is tested to determine if an ejection occurs through one of the processes. In case ejection processes compete, a random selection of the process leading to an effective ejection is carried out. The Na source term intensity is set to be cell dependent in order to investigate different surface distributions.

3. Simulation Results

[10] We have investigated the potential origins of the exospheric emission and of its variation by changing:

[11] 1) the spatial distribution of the fraction of non ice contaminants f_{nonice} in the surface ice (uniform or following *Grundy et al.* [2007]),

[12] 2) the spatial distribution of the Na surface source rate Ψ that is the flux of fresh Na atoms brought to the surface from below (either uniform or correlated with the non ice fraction distribution),

[13] 3) the PSD cross section Q from 10^{-20} cm² to 10^{-19} cm²,

[14] 4) the ratio Y_{ice}/Y_{nonice} between sputtering yields from minerals and from pure ice from $Y_{ice}/Y_{nonice} = 20$ to $Y_{ice}/Y_{nonice} = 40$,

[15] The average Na surface source rate Ψ along one orbit is adjusted in order to match observations. For all simulations the mean sputtering yield Y_{cell} in one cell is given by $Y_{cell} = Y_{nonice} * f_{nonice} + Y_{ice} * (1 - f_{nonice})$ where f_{nonice} is the fraction of non ice material in the cell.

[16] Five representative cases have been studied and are described in Table 1. Cases 1 to 4 relates to steady state plasma conditions at Europa's orbit whereas in case 5 we simulate a local plasma injection at Europa's surface between

midnight and 0300 Jupiter Local Time with a flux of 1.6×10^8 cm⁻².s⁻¹.

3.1. Comparison With Earth Ground Based Observations

[17] Figure 1 shows the calculated sodium emission at 3 Europa radii from Europa's surface for cases 1 to 5 as a function of Europa phase angle, together with the integrated intensity observed at the same position on the 11/28/2000, 11/29/2000, and 11/30/2000. For all the simulated cases, a minimum surface source term of at least 3×10^6 cm⁻² s⁻¹ had to be assumed in order to obtain a good agreement between calculated and observed exospheric emission intensities at phase angles of 288° and 129°. This source rate intensity is in good agreement with *Leblanc et al.* [2002].

[18] For cases 1 to 4, the global variation of the simulated emission is by up to a factor of 10, but is not large enough to reproduce the emission intensity observed at a phase angle

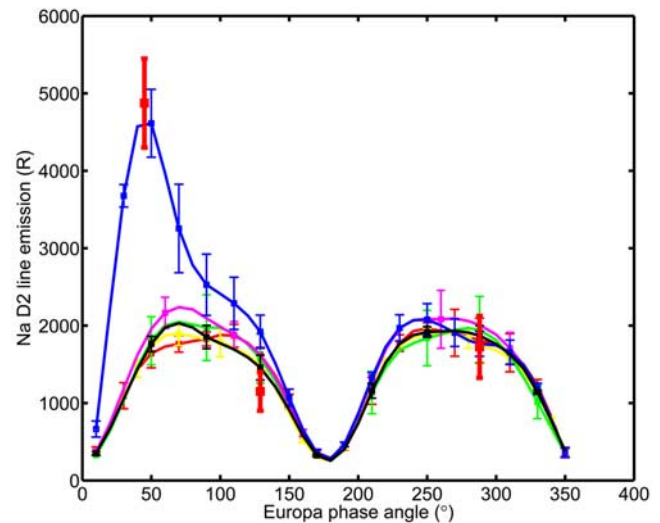


Figure 1. Simulated sodium emission brightness for cases 1 to 5 as a function of Europa phase angle. The dispersion between Eastward, Westward, Northward and Southward integrated emission brightnesses observed at 3 radii from Europa's surface is represented by bars on the curves. The numerical noise of our calculation is at most of the same order. Red line: case 1, green line: case 2, magenta line: case 3, black line: case 4, and blue line: case 5. The integrated intensity observed at 2'' (same distance) from Europa's disk center (average between 2'' East, West, North, and South) on the 11/28/2000 (mean phase angle close to 288°), 11/29/2000 (mean phase angle close to 45°), and 11/30/2000 (mean phase angle close to 129°) is also shown in horizontal red lines with bars.

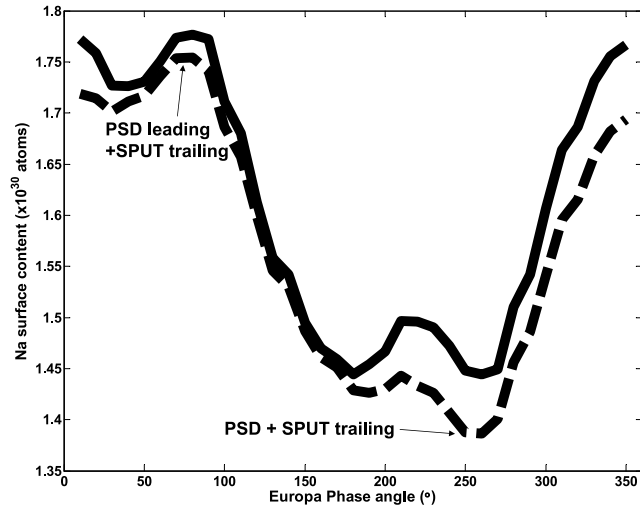


Figure 2. Variations of the dayside Na content (in 10^{30} Na atoms) along Europa orbit. Case 1: solid line and Case 3 dashed line.

of 45° . The emission varies from about 250 Rayleigh (R) when Europa's positions are close to 10° before or after the occultation to about 2000R at phase angles of 90° and 270° . Both brightness decreases observed around 180° and 0° phase angles are due to the decrease of the solar photon flux exciting the sodium emission lines when the Doppler shift of the sodium atoms with respect to the Sun is minimized. Clearly from cases 1 to 4 in Figure 1, the global circulation of the sodium atoms cannot induce the observed peak of brightness at 45° phase angle as suggested by *Leblanc et al.* [2005].

[19] Except in cases 3 and 4, no emission asymmetry between Eastern and Western parts of Europa's orbit is observed. When the PSD cross section is increased by a factor 10 with respect to the nominal value (magenta line case 3), a slight emission bump appears around 70° . A decrease of the sputtering yield from ice, resulting in an increase of the sodium ejection rate through PSD, produces the same effect (black line case 4). However, cumulating those two effects does not result in a significant emission enhancement. Comparison of our model outputs with measured emission at 6 and 8 Europa radii (not shown here) on the 11/28/2000 and 11/30/2000 are also in good agreement, with an average root mean square error of 250R over the two dates, indicating that the energetic part of the energy distribution of the ejected sodium is correctly modelled.

3.2. Surface/Exosphere Related Signatures

[20] As can be seen in Figure 1, excluding case 5, there is actually slightly better agreement between the observed and modelled dispersion of the emission intensities between East, West, North and South sides of Europa (bars in Figure 1) when the Na source term is distributed as the non ice fraction published by *Grundy et al.* [2007] (case 2), than when a uniform distribution over the surface is assumed (cases 1, 3, and 4). This result suggests a supply of Na from the subsurface peaking on Europa's trailing hemisphere. Such enhancement could be driven for instance by diffusion of alkali induced by charged particle irradiation of the surface [*Johnson and Baragiola*, 1991]. A non uniform distribution

of the Na surface source may therefore induce significant exospheric spatial heterogeneities.

[21] Figure 2 shows that the dayside is globally enriched when Europa travels from 0° to 90° phase angles (where sputtering acts mainly on the nightside), before being depleted until its content reaches a minimum around 270° (where both PSD and sputtering act on the dayside). Those variations by up to 25% of the dayside sodium content are fully consistent with a global redistribution of the surface sodium from trailing to leading hemispheres induced by ion sputtering. The local minimum at 40° and maximum at 220° of the dayside surface content result from the motion of the peak of surface density associated with rich non-ice surface regions concentrated on the trailing hemisphere [*Grundy et al.*, 2007] from day to night sides (Figure 3). Indeed no extrema at 40° and 220° are observed when we simulate an exosphere associated with a uniform non-ice surface content. An increase of the PSD cross section decreases the surface content in case 3 compared to the nominal case 1 by about 2% to 3% of the mean content and leads to an increased exospheric content consistent with the increased emission brightness observed in case 3 compared to case 1. The presence of an emission bump around 70° (Figure 1) not seen in case 1, suggests that the desorption time due to PSD after the occultation is too large to produce a peak around 45° . The amplitude of variation of the dayside surface content during one orbit is $\sim 9\%$ larger in case 3 than in case 1 due to an increased circulation from trailing to leading.

[22] When the sodium source term is uniformly distributed over the surface (case 3), the surface density inhomogeneities displayed in Figure 3 are mainly due to variations of the mean sputtering yield with the surface composition (lower on the trailing hemisphere), the geometry of the impacting flux (peaking on the trailing hemisphere), and the sodium redistribution including re-ejection due to PSD from the leading side (slightly increasing the density on the trailing hemisphere). At 130° phase angle, the trailing surface content has globally increased by up to 2% of the

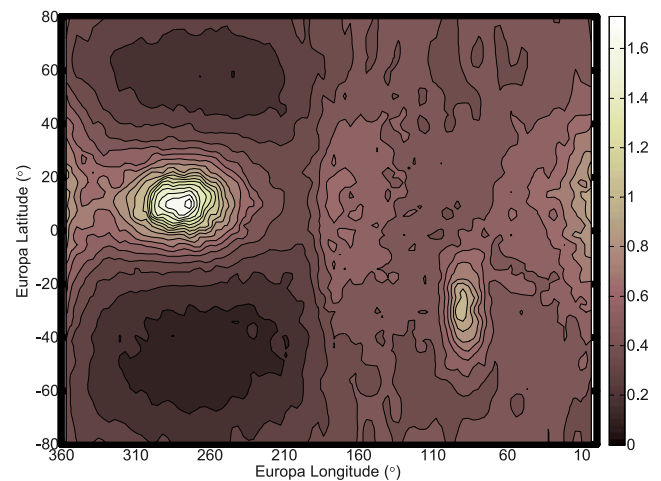


Figure 3. Na surface density (in 2×10^{13} Na/cm $^{-2}$) calculated for case 3 when Europa phase angle is 130° (11/30/2000 observations). At this date dayside longitudes extend from 50° to 230° . The trailing hemisphere apex is located at (0° , 270°).

averaged density compared to 270° , which appears to be a direct consequence of PSD acting over the leading hemisphere after the occultation. We obtain a relatively slight depletion of the surface content (by 10% with respect to the average density) near equatorial regions facing Jupiter or centered on the southern leading hemisphere (Figure 3), consistent with ice dominated regions with higher sputtering yield compared to other regions. Large sodium depletion ($> 80\%$ with respect to the average) is mainly seen to occur in northern and southern areas over the trailing hemisphere. Though the region near the apex of the trailing hemisphere receives the largest amount of radiation, its lower sputtering yield compared to that of regions with higher ice content results in sodium enrichment by up to 60% of the average density.

[23] Due to the surface inhomogeneities visible on Figure 3, density increases are seen in the exosphere at 150 km altitude. Such signatures of surface heterogeneities disappear above 300 km. By comparing variations of mean exospheric densities in a large range of latitudes along one Europa's orbit, we observe for cases 2 and 3 clear asymmetries between leading and trailing exospheric contents depending on Europa's orbital position. In particular in case 3, the day/leading hemisphere densities are larger than the night/trailing densities by up to a factor 2 at 150 km, equatorial latitude and 50° phase angle, whereas the situation is reversed at 270° phase angle. In case 2, exospheric densities are larger over the trailing hemisphere after the occultation, due to a Na surface source term peaking on the trailing, whereas this trailing/leading asymmetry disappears after noon, due to the simultaneous action of PSD and sputtering over the trailing hemisphere. Such trailing/leading and day/night asymmetries observed in cases 2 and 3 suggest that density ratios between leading/trailing and day/night hemispheres can give relevant information on the dominant ejection process and on the Na source distribution at the surface.

3.3. Model for Enhanced Emission Brightness

[24] Sputtering typically dominates the Na surface ejection rate by more than one order of magnitude. In most cases we observed that the photo stimulated desorption contribution increased after the occultation, when Europa phase angle varies from 0° to 180° , then decreased during the other half of the orbit, consistent with the night hemisphere enrichment and dayside depletion. Moreover, from 0° to 180° phase angle, PSD and sputtering act mainly on different hemispheres and do not fully compete. This is in contrast to the portion of orbit from noon to midnight, where the PSD ejection rate decreases, due to sodium depletion in the dayside surface, and its competition with sputtering. An emission enhancement of the same amplitude as that observed on the 11/29/2000 would require a dayside sodium enrichment of 200% through sodium redistribution before Europa's occultation. Such an enrichment would correspond to $\sim 2.8 \times 10^{30}$ atoms migrating from the trailing side to the leading side between 180° and 10° phase angle. The average ejection rate due to sputtering of about $1.5 \times 10^7 \text{ cm}^{-2} \cdot \text{s}^{-1}$ corresponds to less than 3.5×10^{29} atoms released in the exosphere during half Europa rotation, from which only a part of the distribution can

potentially reach the opposite hemisphere and be trapped in the regolith. Therefore a global trailing to leading migration of the Na sodium cannot explain the observed emission enhancement.

[25] Fresh injections of ions and electrons from the outer magnetosphere, which have been reported based on Galileo EPD data [see, e.g., *Mauk et al.*, 1999], may produce significant variations of the exospheric content. In particular the blue curve on Figure 1 (case 5) show the emission variability obtained by simulating an increase by a factor of 8 of the incident ion flux intensity at the surface (that is $1.6 \times 10^8 \text{ cm}^{-2} \cdot \text{s}^{-1}$), starting when Europa passes through Jupiter magnetotail and during the first eighth of the orbit (10.6 hours). Such injection corresponds to about 9.35×10^{29} magnetospheric particles impacting Europa's surface. Typical hot plasma injections described by *Mauk et al.* [1999] have times scale of 0.5 to 6 hours with azimuthal drift times up to 12 hours, in the range of our estimation. Moreover, energy time dispersed structures analyzed by those authors show increases of the particle flux intensities as energy and species dependent. Variations of the energetic ion flux intensity by factor of 5 have been also reported in *Paranicas et al.* [2002], using Galileo data upstream of Europa between 1997 and 2000. Therefore, a variation of the impacting ion flux by a factor of 8 is in good agreement with expected variations of the ambient plasma intensity at Europa.

4. Discussion and Conclusion

[26] We investigated the observed variations of the emission of sodium in the exosphere of Europa during its orbit around Jupiter. The comparative study of sputtering and PSD ejection processes indicates that PSD alone can not account for the typical emission variations reported by *Leblanc et al.* [2005]. A minimal Na source term of $3 \times 10^6 \text{ cm}^{-2} \cdot \text{s}^{-1}$ is required to produce the average emission intensities observed at different positions around Jupiter. The spatial distribution of the ejected material does not significantly influence the average emission above 4000 km along Europa's orbit for a uniform Na surface source term distribution. At altitudes typically lower than 500 km, the non-uniformity of the surface content produces clear asymmetries between trailing and leading hemispheres exospheric densities. Temporal variation of the impacting flux intensity due to plasma injection may also cause large variations in the emission intensity. A transient increase of the ion flux impacting the surface by a factor of 8 during 10 hours would explain the enhanced emission observed on the 11/29/2000 [*Leblanc et al.*, 2005]. Compositional and energetic structures of the impacting flux have now to be investigated through data analysis and further modelling. The duration of the simulated event suggests an injection occurring farther out from Europa's orbit and diffusing in. A similar enhancement should be observed for the whole Europa's atmosphere, which should have very variable density, composition and 3D structure along its orbit around Jupiter. Since sodium emission lines can be observed from the Earth and since a large variability in emission brightness can be expected, such observations could be useful to improve our model and prepare future missions towards the Jupiter system.

References

- Brown, M. E. (2001), Potassium in Europa's atmosphere, *Icarus*, *151*, 190–195.
- Brown, M. E., and R. E. Hill (1996), Discovery of an extended sodium atmosphere around Europa, *Nature*, *380*, 229–231.
- Cassidy, T. A., R. E. Johnson, M. A. McGrath, M. C. Wong, and J. F. Cooper (2007), The spatial morphology of Europa's near-surface O₂ atmosphere, *Icarus*, *191*, 755–764.
- Cooper, J. H., R. E. Johnson, B. H. Mauk, and N. Gehrels (2001), Energetic ion and electron irradiation of the icy Galilean satellites, *Icarus*, *149*, 133–159.
- Grundy, W. M., et al. (2007), New Horizons mapping of Europa and Ganymede, *Science*, *318*, 234–237.
- Johnson, R. E. (2000), Sodium at Europa, *Icarus*, *143*, 429–433.
- Johnson, R. E., and R. A. Baragiola (1991), Lunar surface: Sputtering and secondary ion mass spectrometry, *Geophys. Res. Lett.*, *18*, 2169–2178.
- Leblanc, F., and R. E. Johnson (2003), Mercury's sodium exosphere, *Icarus*, *164*, 261–281.
- Leblanc, F., R. E. Johnson, and M. Brown (2002), Europa's sodium atmosphere: An ocean source?, *Icarus*, *159*, 132–144.
- Leblanc, F., A. E. Potter, R. M. Killen, and R. E. Johnson (2005), Origins of Europa Na cloud and torus, *Icarus*, *178*, 367–385.
- Mauk, B. H., D. J. Williams, R. W. McEntire, K. K. Khurana, and J. G. Roederer (1999), Storm-like dynamics of Jupiter's inner and middle magnetosphere, *J. Geophys. Res.*, *104*, 22,759–22,778.
- Paranicas, C., J. M. Ratliff, B. H. Mauk, C. Cohen, and R. E. Johnson (2002), The ion environment near Europa and its role in surface energetics, *Geophys. Res. Lett.*, *29*(5), 1074, doi:10.1029/2001GL014127.
- Yakshinskiy, B. V., and T. E. Madey (1999), Photon-stimulated desorption as a substantial source of sodium in the lunar atmosphere, *Nature*, *400*, 642–644.

F. Cipriani and O. Witasse, ESTEC, ESA, PB 299, NL-2200 Noordwijk AG, Netherlands. (fcipriani@rssd.esa.int)

F. Leblanc, Osservatorio Astronomico di Trieste, Via Tiepolo 11, I-34143 Trieste, Italy.

R. E. Johnson, Engineering Physics, University of Virginia, Thornton Hall B103, Charlottesville, VA 22903, USA.